Spectroscopic and microscopic characterization of porphyrin-carbon nanostructures interactions in the presence of metal nanoparticles

Leticia Verbustel
Instituto Superior Técnico - Lisbon U.

Abstract—The objective of this study was to produce stable nanohybrids made of four different porphyrins (meso-tetra(4-N-methyl-pyridyl)porphine, TMpyP, meso-tetrakis(p-sulfonatophenyl)porphyrin, TSPP, zinc tetramethylpyridylporphyrin, ZnTMpyP, and tetraphenylporphine, TPP) and three carbon based nanostructures (functionalized single wall carbon nanotubes, fCNT, multi wall carbon nanotubes MWCNT, and functionalized graphene sheets, fGRAPH), with and without decoration of gold nanoparticles (AuNP). The interactions were investigated using UV/vis absorption, steady-state and time-resolved fluorescence. Microscopic techniques such as Fluorescence Lifetime Imaging Microscopy (FLIM) and Transmission Electron Microscopy (TEM) were also employed to characterize the morphology of deposited samples.
Porphyrin/fCNT nanohybrids could be produced and complexes were observed with porphyrins of opposite sign. The carbon based nanostructures fGRAPH and MWCNT did not result in the same which points out the importance of electrostatic interactions. No differences could be detected upon decoration of MWCNT with AuNP produced in two different ways: preformed and *in situ*. However, FLIM images obtained for deposited samples showed fluorescence quenching of the porphyrin with the addition of preformed AuNP, whereas for the *in situ* AuNP an enhancement of the porphyrin fluorescence intensity together with a decrease of its lifetime was observed, characteristic of the MEF effect.

Index Terms—Porphyrins, carbon based nanostructures (CBN), gold nanoparticles (AuNP), steady-state and time-resolved fluorescence, sensors

1 Introduction

Carbon based nanostructures (e.g. carbon nanotubes and graphene sheets) have very attracting electronic properties, outstanding mechanical strength and an impressive surface area. These characteristics make carbon based nanostructures (CBN) interesting materials in the context of energy conversion. [1] An important aspect is the ability of these materials to noncovalent bind to aromatic organic molecules (pyrene, fluorescein, porphyrin, etc.) through π-π interaction, making it of interest in many applications such as for tuning electronic and transport properties and for adsorbing and removing dye pollutants in the treatment of wastewater. [2]
In this research, porphyrins are used as aromatic molecules. These two-dimensional aromatic systems also possess very interesting optical, photophysical, photochemical and electrochemical properties. [3]–[5]

In this report, the focus is to understand more the interaction behaviour between the aromatic porhyrin and CBN. Four different porphyrins were used in combination with three different CBN. Also investigated were the interactions between hybrid systems of the same four porphyrins and gold nanoparticles (AuNP) adsorbed to a chosen CBN. AuNP is added because it is known to help prevent aggregation of the CBN and additionally adds more stability and functionality to the systems.

L. Verbustel is with the University of Antwerp, dept. of Applied Engineering: Chemistry, this work was done at Centro de Química Estrutural, Complexo I, Instituto Superior Técnico, Universidade de Lisboa, Av. Rovisco Pais, 1049-001, Lisboa, Portugal.
E-mail: leticia.verbustel@student.uantwerpen.be

2 Experimental section

2.1 Materials

The used solvents and chemicals were from spectrophotometric grade and used as obtained from the manufacturer. Functionalized graphene and ZnTMpyP were homemade and prepared elsewhere. [6], [7] Table 1 gives both the molar extinction coefficient ϵ found in literature and ϵ determined experimentally of the used porphyrins. Either distilled or ultrapure water was used for making stock solutions.

TABLE 1: Comparison of the experimental ϵ and the ϵ found in the literature [8], [9]

Porphyrin	ϵ_{lit} // $\epsilon_{exp}(.10^5 M^{-1}.cm^{-1})$	λ (nm)
TMpyP	2,26 // 1,97 (water), 2,16 (DMF)	422
ZnTMpyP	2,21 // 1,88	437
TSPP	5,1 // n.a.	413
TPP	4,2 // n.a.	418

For all the measurements, the porphyrin concentration was kept constant (2 μM) while the concentration of CBN was changed. From the stocksolutions the desired concentrations were diluted using the appropriate solvent (distilled or ultrapure water, DMF, buffer and/or a mixture). A separate sample containing the highest concentration of CBN but without porphyrin was prepared for comparison.

2.2 Synthesis of AuNP and its adsorption to CBN

Citrate-capped AuNP can be obtained by a chemical reduction of a metal precursor salt, here tetrachloroaurate(III), which is induced with sodium citrate. AuNP were synthesised in two different ways: preformed and *in situ*. When using the preformed method, the gold nanoparticles are made separately and later mixed with the already prepared CBN, whereas with the *in situ* method AuNP is simultaneously prepared with the CBN. Additionally for both methods, poly(ethylene glycol) or PEG could be added to ease solubility and dispersion in solution.

2.3 Instrumentation

A PerkinElmer Lambda 35 spectrophotometer was employed in UV-vis absorption measurements. The bandwidth was set to 1 nm for every experiment, wavelengths ranged from 800 to 300 nm. Background scattering of the absorption spectra was corrected by $corr(\lambda) = \frac{a}{\lambda^b} + c$, in which λ is the wavelength of the incident radiation, whereas a, b, and c are empirical parameters. [10], [11] Steady-state fluorescence spectra were obtained with a SPEX® Fluorolog® Tau-3 spectrofluorometer (HORIBA Jobin Yvon) in FL3-11 configuration. The used lamp source, a 450 W Xenon lamp, had to be stabilized for at least 30 minutes before measurements. Fluorescence emission spectra were measured between 580 and 850 nm, at a excitation wavelength that takes into account the prevention of inner filter effects. The instrumental response was corrected by means of a correction function provided by the manufacturer. All spectra were recorded at room temperature by using a quartz cuvette with 1 cm path length.

Fluorescence lifetimes were also obtained with the SPEX® Fluorolog® Tau-3 spectrofluorometer (HORIBA Jobin Yvon) in FL3-11 configuration with a NanoLED pulse diode as a light source. Decays are automatically fitted with reconvolution of a profile of the light source, which is the prompt using the light-scattering standard LUDOX® with a lifetime of 0 ns. [12] With the aid of the program DAS6 the decays are fitted once more, from which the goodness of the fit was evaluated by the usual statistical criteria and by visual inspection of the weighted residuals distribution. The average lifetime τ_{av} was than calculated by $\tau_{av} = \frac{\sum A_i.\tau_i^2}{\sum A_i.\tau_i}$.

FLIM measurements were obtained with a time-correlated single-photon counting (TCSPC) technique using commercial equipment (Microtime 200 from PicoQuant). A 635 nm pulsed picosecond diode laser was used as light for the excitation, a single photon avalanche diode performed the detection and the data was processed by a special TCSPC board. Before adding some drops of the sample, the used glass slides were submerged for a minimum of five hours in freshly prepared Piranha solution (H_2O_2:H_2SO_4 = 1:3), washed with distilled water and dried one by one using N_2-gas. This procedure makes the surface of the glass slides hydrophilic.

TEM images were obtained with a Hitachi H-8100 electron microscope. Some quickly evaporating solvent, usually ethanol, is added to a small amount of solid material. From this sample solution, a small drop was deposited and air-dried on a carbon/Formvar-coated copper grid before executing the experiment.

2.4 Data analysis

2.4.1 Determination of K_a

When there is evidence of a complex in the absorption spectrum, the binding or association constant K_a can be calculated using the next equation [S.M. Andrade]:

$$A_T(\lambda) = [Porf]_0 \frac{\epsilon_p(\lambda) + \epsilon_c(\lambda) K_a [CBN]^n}{1 + K_a [CBN]^n} \quad Eq.1$$

in which $A_T(\lambda)$ is the fitted absorbance at measured wavelength λ, $[Porf]_0$ is the begin concentration of the porphyrin = 2 μM, $\epsilon_p(\lambda)$ and $\epsilon_c(\lambda)$ are the extinction coefficients of respectively the porphyrin monomer and complex at measured wavelength λ, $[CBN]$ is the concentration of CBN, and n is the term that gives an idea of the process, whether there is cooperativity or not (n=1 when no cooperativity, 1:1 complex). By optimising the fit using MS Excel, K_a can be calculated.

2.4.2 Determination of K_{SV} and k_q

From fluorescence emission and fluorescence lifetime measurements the Stern-Volmer quenching constant K_{SV} and the bimolecular quenching constant k_q can be calculated using the Stern-Volmer equation:

$$\frac{I_0}{I} = (1 + K_S[Q])(1 + K_{SV}[Q]) \quad Eq.2$$

with K_{SV} being equal to $k_q.\tau_0$, I_0 and I are the fluorescence intensities of the fluorophore in respectively the absence and the presence of the quencher, $[Q]$ is the concentration of the quencher and K_S is the static quenching constant.

For high concentrations of quenchers static quenching may occur even though no complex is formed. This is due to close distance between the fluorophore and the quencher. According to this model the quencher remains nearby the fluorophore in a sphere at the moment of excitation instead of forming a complex. Based on Poisson distribution, for this model, a modified Stern-Volmer equation is used:

$$\frac{I_0}{I} = (1 + K_{SV}[Q]).e^{V[Q]} \quad Eq.3$$

with V being the static quenching constant, which represents the volume of the sphere. [2], [13], [14]

3 Results and Discussion

3.1 Porphyrin interaction with CBN

3.1.1 Porphyrin - fCNT interaction in aqueous solution, in DMF and in buffer

A. *TMpyP*

The normalized UV/vis absorption spectrum (fig. 1(a)B) shows a red shift of the Soret band with increasing amount of fCNT/water, from 422 to 444 nm, which is accompanied by a broadening of the band. The red shift of the Soret band is usually connected with

- Protonation of the porphyrin pyrrole nitrogens.
- Formation of porphyrin J-aggregates
- Formation of porphyrin/SWNT self-assemblies.

Protonation of the porphyrin ring can be excluded due to the lack of a change in number of Q-bands, which would have been reduced from 4 to 2. The band shows a widening instead of a narrowing, which one would expect in the case of formation of J-aggregates, and thus this option can also be excluded. Therefore, the changes in the spectrum can be assigned to the formation of porphyrin/SWCNT self-assemblies or complexes. [15], These complexes are noncovalently bonded through π - π interactions and/or by electrostatic interactions, which take place between monomeric TMpyP and fCNT.

When using DMF as a solvent, the normalized UV/vis absorption (fig. 1(b)B) also shows a red shift of the Soret band with increasing amount of fCNT/DMF, going from 425 to 431 nm, again accompanied by a widening of the band.

When comparing the systems, it can be seen that the red shift is smaller (a difference of 6 nm vs. 22 nm), plus the broadening of the band is less pronounced in the case of DMF. The conclusion can be made that also here the change in spectrum can be assigned to self-assemblies between TMpyP and fCNT, but the responsible π - π interactions are not as strong as in water and electrostatic interactions are probably absent in the case of DMF.

The binding constant K_a has a value of 61,7 mL/mg and 93,1 mL/mg for TMpyP and fCNT in water and in DMF, respectively (calculated using Eq. 1). Even though the interactions between porphyrin and CBN were less strong in the case of DMF according to the absorption spectra, K_a values show that the binding capability between TMpyP and fCNT is higher in DMF, yet they are in the same order of magnitude.

The fluorescence spectrum TMpyP/water (fig. 2A) shows one, almost structureless emission band (λ_{max} ~713 nm), while the spectrum of TMpyP/DMF (fig. 2B) contains two vibrational resolved emission bands (λ_{max} ~654 and ~718 nm). According to Vergeldt F.J. *et al.* [16] this difference is due to an intramolecular mechanism involving mixture between the first excited state, S_1, and a nearby CT (charge-transfer) state.

The fluorescence intensity of (A) first increases a little, where after it drops with the further increase of fCNT/water. The intensity of (B) decreases immediately

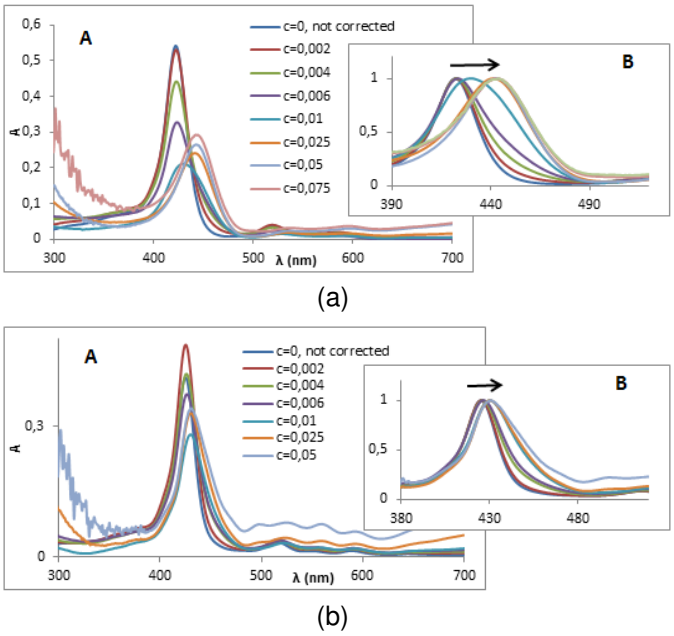

Fig. 1: UV/vis absorption spectrum (A) and normalized spectrum (B) of TMpyP (2 μM) upon addition of fCNT in water(a) and in DMF(b)

with the increase of fCNT/DMF. Neither of the spectra show any other changes, i.e. formation of a new emission band, although in both cases there was a red shift in the absorption spectra, suggesting the existence of a complex (see above). This result indicates that both the TMpyP/fCNT-complexes in water and in DMF do not emit and the changes in the emission spectra are due to the TMpyP monomer.

The Stern-Volmer quenching constant K_{SV} can primarily be assessed from lifetime measurements made in the absence and in the presence of the quencher. The lifetimes however are not influenced much.

Using DMF as a solvent, a very low value for K_{SV} is obtained, and therefore it is plausible to also exclude the dynamic contribution to the quenching process. The confirmation has to be made based on fluorescence lifetime measurements (see ahead).

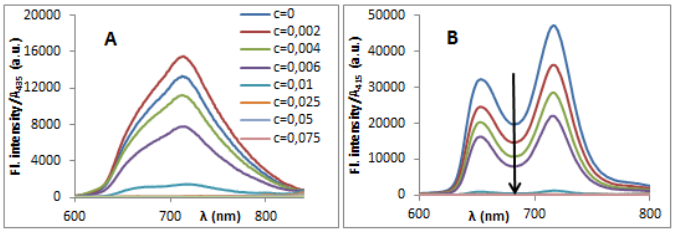

Fig. 2: Fluorescence emission spectra of TMpyP (2 μM) with increasing concentration of fCNT in (A) water and (B) DMF (0-0,075 mg/ml); λ_{exc} = 435 and 415 nm, respectively

Fluorescence decays (fig. 3) are fitted using two exponentials in both the absence and the presence of fCNT, having a average lifetime, τ_{av}, of ~4,96 ns for TMpyP in water. Since the lifetime values stay consistent, this

confirms that the TMpyP-fCNT complex must be not fluorescent or has a fluorescence quantum yield much lower than that of the monomer and therefore it is not detectable for the low quencher concentrations used to obtain the quenching parameters. (Note that measurements with higher $[Q]$ were not possible to be made, due to the low intensity of such samples under the laser power excitation available.)

In the absence of fCNT/DMF the average lifetime has a value of 7,63 ns, fitted using three exponentials. Upon addition of fCNT/DMF, the lifetimes increases untill ∼9,98 ns, also fitted with three exponentials. Since there is no dependence on the amount of fCNT added and the fluorescence spectrum showed no proof of a complex, the complex TMpyP-fCNT in DMF is not fluorescent, likewise to the complex in water.

Noticeable is the dependence of lifetime measurements towards their environment: the lifetimes obtained in DMF are notably higher than the ones obtained in water, one reason being the difference in the polarity/polarizability of the two solvents.

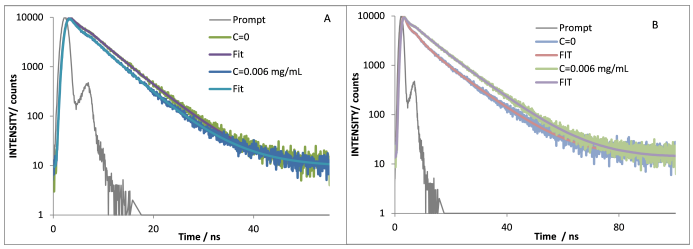

Fig. 3: Fluorescence decays of TMpyP (2 μM) without and with fCNT (0.006 mg/mL) in A) water and B) DMF; λ_{exc} = 445 nm, λ_{emi} = 710 nm

B. *ZnTMpyP*

The normalized UV/vis absorption of ZnTMpyP/water (fig. 4B) also shows a red shift of the Soret band with increasing amount of fCNT/water, going from 436 to 459 nm. This shift is accompanied by a widening of the band. The change in the spectrum can be assigned to self-assemblies between ZnTMpyP and fCNT, likewise to TMpyP and fCNT.

The K_a value of ZnTMpyP is quite high, ∼870 mL/mg. This suggests a great ability of fCNT to form assemblies with ZnTMpyP.

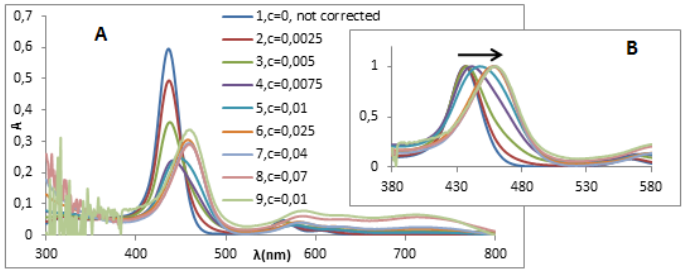

Fig. 4: UV/vis absorption spectrum (A) and normalized spectrum (B) of ZnTMpyP/water (2 μM) upon addition of fCNT/water

Again here, the fluorescence intensity of ZnTMpyP/water lowers with increasing concentration of fCNT/water (fig. 5). This is followed by changes in the relationship between the two vibronics, which points to the formation of an emissive ZnTMpyP/fCNT complex. Confirmation can be obtained from fluorescence lifetimes.

Addition of fCNT up to 0.0075 mg/mL does not lead to significant changes in τ_{av} of ZnTMpyP (table 2). However, above this concentration, there is a clear increase of this parameter at the expenses of the increasing contribution of a longer lifetime component of ∼5 ns, which can be tentatively assigned to the emission of the complex, which was possible to detect at higher quencher concentrations where you have more complex formed, by contrast to the case of TMpyP, shown above.

Eq. 2 was used to obtain the rate constants for the quenching process. K_{SV} has the value of 0 mL/mg due to no decrease in the fluorescence lifetimes. As for the static quenching, K_a, using the value of K_a obtained from absorption data (K_a being ∼870 mL/mg), the equation can describe the quenching effect only up to 0.01 mg/mL of fCNT. Above this quencher concentration the values of I_o/I obtained are much higher than those predicted by Eq. 2. At these quencher concentrations we are in the range where quencher and fluorophore have similar concentrations and therefore there is no longer a linear relationship.

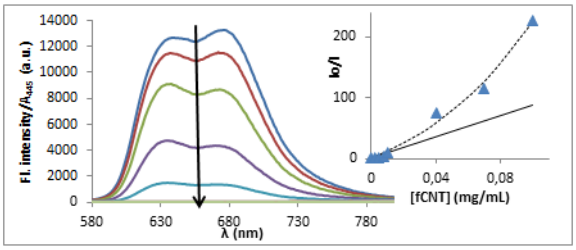

Fig. 5: Fluorescence emission spectrum of ZnTMpyP/water (2 μM) with increasing concentration of fCNT/water (0-0,1 mg/ml); λ_{exc} = 445 nm. Inset: Fitting data of fluorescence quenching for ZnTMpyP with fCNT using Eq. 2

C. *TSPP*

Upon addition of fCNT/buffer, a shoulder appears in the spectrum at around 435 nm (fig. 6). This is also the peak for the di-acid species of TSPP, which is formed upon acidification. The increase of this new band is accompanied by the decrease of the Soret band, located at 414 nm. At ca. 422 nm, an isosbestic point is observable. If these changes were related with formation of the di-acid species, this would mean that due to symmetry changes, the absorption spectrum would change from 4 Q-bands to 2 Q-bands upon addition of fCNT. However, due to the increase of solution scattering in that region, together with the very low extinction coefficient of such bands, we cannot conclude anything.

Assuming the possibility of a complex, K_a has a

TABLE 2: Fluorescence lifetimes of ZnTMpyP/water (2 μM) with fCNT in water; λ_{exc} = 445 nm, λ_{emi} = 630 nm

[fCNT/water] mg/mL	F_1	τ_1 (ns)	F_2	τ_2 (ns)	F_3	τ_3 (ns)	τ_{av} (ns)	XSQ
0	0.74	1.38	0.26	0.533	-	-	1.28	0.889
0.0025	0.67	1.43	0.33	0.858	-	-	1.30	0.958
0.005	0.45	1.51	0.55	0.953	-	-	1.27	0.963
0.0075	0.35	1.59	0.65	0.968	-	-	1.26	1.19
0.01	-	-	0.98	1.17	0.02	4.87	1.45	1.20
0.025	-	-	0.93	1.29	0.07	4.76	2.01	1.21
0.05	-	-	0.86	1.22	0.14	5.00	2.76	1.19

value of ~37,9 mL/mg. Therefore, only about 20 % transformation of 2 μM TSPP is caused by 0,07 mg/mL of fCNT/buffer.

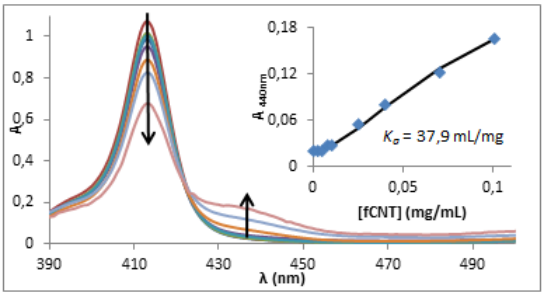

Fig. 6: UV/vis absorption spectrum of TSPP/water (2 μM) upon addition of fCNT/buffer (0-0,07 mg/ml). Inset: dependence of TSPP absorbance at 440 nm on [fCNT]. The line represents the fit of Eq. 1; pH=7.4

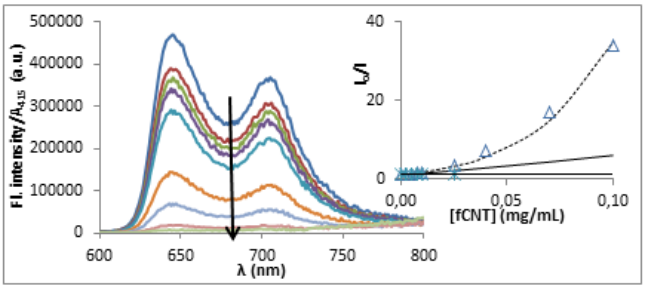

Fig. 7: Fluorescence emission spectrum of TSPP/water (2 μM) with increasing concentration of fCNT/buffer (0-0,1 mg/ml); λ_{exc} = 415 nm. Inset: Fitting data of fluorescence quenching for TSPP with fCNT using Eq. 2

The higher the concentration of fCNT/buffer which is added to TSPP, the lower the fluorescence intensity until the curves maximum peaks flatten completely (fig. 7). The absence of an additional peak at ~674 nm [17] indicates that the new absorption band at 435 nm (see above) is probably not due to the di-acid porphyrin but due to a complex which is non fluorescent and therefore, the emission obtained is due to TSPP monomer.

The lifetime of TSPP obtains a value of 9,53 ns, which systematically decreases until 9,12 ns. The number of exponentials needed for the fitting stays the same (2) suggesting no second species emits, meaning the complex is non emissive. The systematic decrease in lifetime suggests dynamic quenching takes place. Furthermore, there is no evidence for the formation of the di-acid species which has a fluorescence lifetime of ~3.8 ns.

Using Eq. 2, a value of 48.5 mL/mg could be obtained for K_a, which is in line with the value obtained using absorption data. On the other hand, K_{SV} has a much higher value than that obtained with fluorescence lifetimes (K_{SV} ~1.7 mL/mg). Attention should be pointed out to the different range of concentrations used in lifetime measurements.

If we keep K_{SV} constant and equal to that obtained through lifetime measurements (~1.7 mL/mg) and use K_a ~38 mL/mg withdrawn from absorption data, then we can only describe the quenching process until up a concentration of 0.025 mL/mg of fCNT (full black line, inset fig. 7). Again, the experimental values are much higher than those predicted by Eq. 2.

D. *Comparison*

The three porphyrins used (TMpyP, ZnTMpyP and TSPP) show interaction in the ground state with fCNT and suggest self-assemblies between porphyrins and fCNT. This conclusion is based on the broadening of the Soret band, which can be interpreted as a sign of the existence of more than one component in the sample. Only TSPP had an isosbestic point, from which a quantification can be made (~20 % transformation). The scattering interference in the UV/vis spectra could be the reason for the absence of an isosbestic point for the other two porhyrins because its account is not straightforward.

In the excited state, however, no changes were observed that suggest a complex exists. Therefore it can be concluded that the complexes are non fluorescent and the emission was solely caused by the porphyrin monomers. This conclusion is confirmed by lifetime measurements, except for the case of ZnTMpyP. For the latter, we may consider the possibility of interaction between the central metal ion and the carboxylic groups of fCNT.

Regarding solvent choice for TMpyP, water is preferred because more changes in the spectra are observed and thus suggesting stronger interactions, e.g. H-bonding and electrostatic interactions.

Based on the K_a values (table 3) the sequence of the ability to bind with fCNT in the ground state is ZnTMpyP > TMpyP/DMF ~ TMpyP/water > TSPP.

TABLE 3: Association constant K_a (obtained using absorption and emission data) and Stern-Volmer quenching constant K_{SV} for different porphyrins with fCNT

	TMpyP/water	TMpyP/DMF	ZnTMpyP	TSPP
K_a - abs (mL/mg)	61.7	93.1	869	37,9
K_{SV} (mL/mg)	0	0	0	1,7
K_a - Flu (mL/mg)	286	83.0	1110	48.5

3.1.2 *Porphyrin - fGRAPH interaction in water/DMF mixtures*

A. *UV/vis absorption spectra*

The UV/vis absorption spectra of TMpyP/water, ZnTMpyP/water, TSPP/water (solutions were made using buffer as solvent) and TPP/DMF, all with a concentration of 2 μM, with increasing concentration of fGRAPH in a water/DMF mixture (2:1), are shown in fig. 8. The Soret bands are located at ca. 422, 440, 415 and 418 nm, respectively. There are small differences in intensity of the peaks and C and D have a small shoulder in the blue region, yet the shape of the bands and their positions did not show any observable changes. Because of these reasons, together with the fact that no new absorption band is formed, one can conclude no interaction occurred between any of the four porphyrins and fGRAPH in the ground state (S_0).

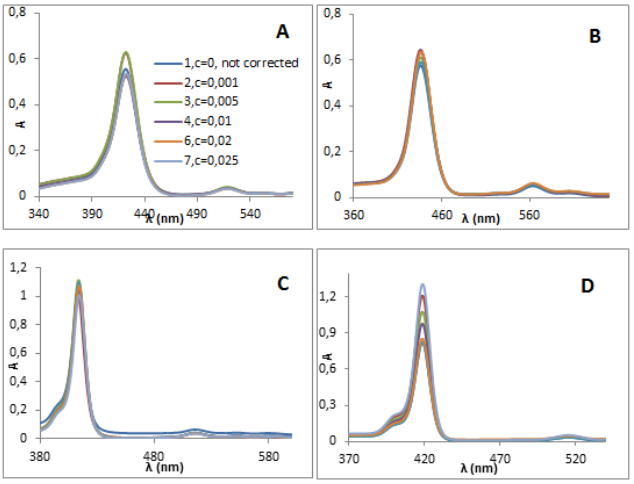

Fig. 8: UV/vis absorption spectra of (A) TMpyP/water, (B) ZnTMpyP/water, (C) TSPP/water and (D) TPP/DMF, all 2 μM, upon addition of fGRAPH/water-DMF

B. *Fluorescence emission spectra*

Noticable in the normalized fluorescence emission spectrum of TMpyP/water (fig. 9(a)) upon addition of fGRAPH/water-DMF is that the spectrum changes from a nonstructured emission band, with its maximum at ca. 712 nm, to two ill-defined vibrational resolved emission bands (λ_{max} ~712 nm and ~658 nm). The bands are changing because the solvent properties are changing as water/DMF is added to the bulk water.

Two peaks at ~636 nm and ~672 nm are detected in the normalized fluorescence spectrum of ZnTMpyP/water with increasing amount of fGRAPH/water-DMF (fig. 9(b)). When fGRAPH/water-DMF increases, there is a small decrease of the left hand peak, together with a 2 nm-shift to shorter wavelengths. Except for the small shift and change in intensity of one of the peaks, nothing changed about the spectrum: no broading, no significant drop in intensity, no formation of a new emission band. This results indicates no interaction occurred in the excited state between the porphyrin and fGRAPH.

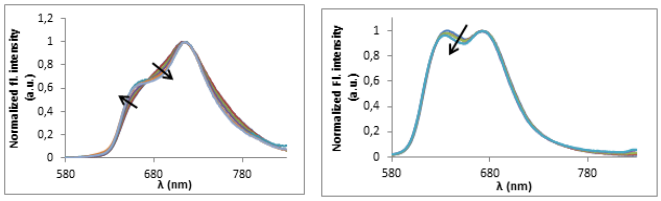

Fig. 9: Normalized fluorescence emission spectrum of (a) TMpyP/water and (b) ZnTMpyP/water, both 2 μM, with increasing concentration of fGRAPH/water-DMF (0-0,025 mg/ml); λ_{exc} = 438 and 454 nm, respectively

With the increase of fGRAPH, the emission intensities of TSPP and TPP (fig. 10) were also increased. Noticeable is that no new emission band appeared, suggesting no complex is formed in the excited state, and hence the emission can be assigned solely to the free porphyrin monomers.

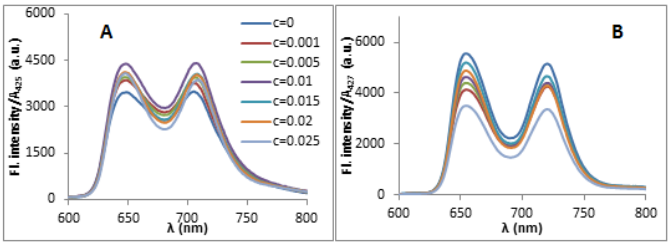

Fig. 10: Fluorescence emission spectra of (A) TSPP/water and (B) TPP/DMF, both 2 μM, with increasing concentration of fGRAPH/water-DMF; λ_{exc} = 425 and 427 nm, respectively.

C. *Lifetime measurements*

Decays concerning TMpyP could be fitted with two or three exponentials, yet the fluorescence spectrum indicated no complex formation. In all three other cases, the fluorescence decays were fitted using just one exponential, suggesting only one emitting species exists. These results confirm that interactions in the excited state of each of the four porphyrins studied with fGRAPH must be much less effective than those evidenced with fCNT.

D. *Comparison*

Figure 11 shows the effect of fGRAPH concentration on the fluorescence intensity ratio of the different porphyrins. The plots of I_0/I vs. C, quencher concentra-

tion, are either close to 1 or decrease below 1, except for ZnTMpyP. Taking into consideration that lifetime measurements gave indication of an absence of dynamic quenching, only for ZnTMpyP we see a decrease in intensity.

As a final remark, it is pertinent to say that although we used a solvent mixture of distilled water and DMF, the availability of fGRAPH towards interaction with porphyrins is probably not as good as for the case of fCNT, which is much more water soluble.

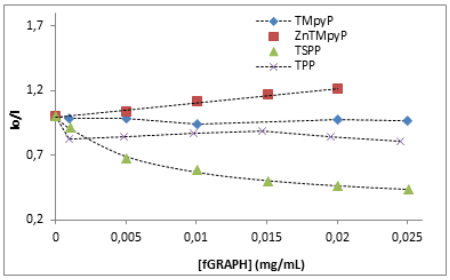

Fig. 11: The plot of intensity quenching upon the quencher concentration C for fGRAPH

3.1.3 Porphyrin - MWCNT interaction in water/DMF mixtures

A. *UV/vis absorption spectra*

The Soret bands of TMpyP/water and ZnTMpyP/water with increasing concentration of MWCNT in a water/DMF mixture (2:1) are located at ca. 425 nm and 439 nm, respectively, as shown in the UV/vis absorption spectra (fig. 12)

There are no changes in the position or the shape of the bands, nor is there a formation of a new absorption band. The conclusion can be made that no complex is formed in the ground state between either TMpyP or ZnTMpyP and MWCNT.

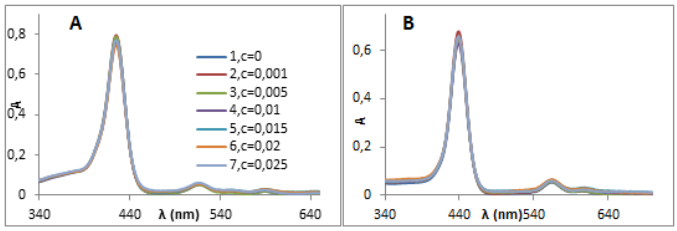

Fig. 12: UV/vis absorption spectra of (A) TMpyP/water and (B) ZnTMpyP/water, both 2 μM, upon addition of MWCNT/water-DMF (in mg/ml)

B. *Fluorescence emission spectra*

There is an significant decrease in fluorescence intensity of TMpyP/water and ZnTMpyP/water upon addition of MWCNT/water-DMF (2:1) (fig. 13) . Except for the drop in intensity, nothing changed about the spectra: the maximum of the peaks stayed the same (A: ~655 and ~717 nm, B: ~630 and ~670 nm) and no new emission band was formed, suggesting no assembly occurred between porphyrin and MWCNT. The emission can be assigned to the free porphyrin monomers.

For TMpyP with MWCNT, the value of K_{SV} is ~0 mL/mg, consistent with the lifetime data (see below) that show independence on the concentration of MWCNT. The static contribution was accounted for by an association constant and the value obtained was K_a ~47.2 mL/mg. In the case of ZnTMpyP interaction with MWCNT there seems to be a concomitant decrease in the fluorescence lifetimes according to the data, but the decrease lies inside the error range of $\pm$ 0.15 (10 %). Taking this result into account, and using Eq.2 for the I_o/I data, a value of 45.1 mL/mg is obtained for the association constant between ZnTMpyP and MWCNT which is quite similar to that obtained with the free-base porphyrin.

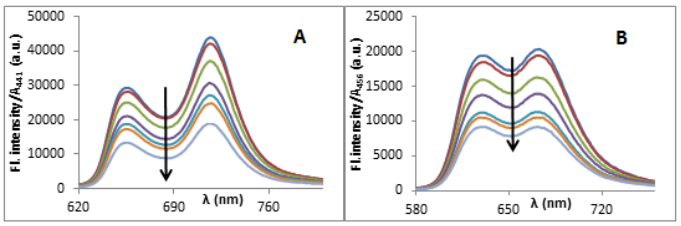

Fig. 13: Fluorescence emission spectra of (A) TMpyP/water and (B) ZnTMpyP/water, both 2 μM, with increasing concentration of MWCNT/water-DMF (0-0,025 mg/ml); λ_{exc} = 441 and 456 nm, respectively

C. *Lifetime measurements*

The fluorescence decay of TMpyP is monoexponential with a lifetime of 11,1 ns. In the presence of MWCNT, the lifetime is lowered to 10,8 ns for all concentration and from which the decays were also fitted by one exponential. Quenching does occur due to the presence of MWCNT, but the lifetimes stay constant, thus there is no proof of a complex, which the fluorescence spectrum already suggested.

The fluorescence decay of ZnTMpyP is also monoexponential with a lifetime of 1,51 ns. The presence of MWCNT lowers the lifetime systematically to 1,45 ns. The decays stay monoexponential. Again here quenching does occur due to the presence of MWCNT, but the lifetimes after addition are consistent inside the margin of error. Therefore, no dynamic quenching was observed.

D. *Comparison*

Based on the plots of F_0/F vs. [MWCNT] of TMpyP and ZnTMpyP (fig. 14), it is hard to say which one has the highest ability of the intensity quenching since the slopes match each other. When comparing the values of K_a (47,2 and 45,1 mL/mg, respectively), it is detected that the values are quite similar and therefore both porphyrins have the same ability to form complexes with MWCNT.

3.1.4 Comparison between CBN

Absorption spectra revealed that strong π-π binding with the ground state (S_0) of the porphyrins occurred for fCNT but not for fGRAPH or MWCNT.

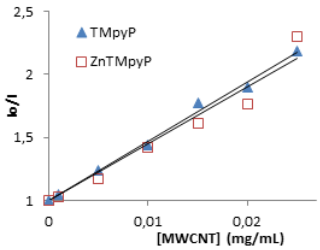

Fig. 14: Plot of changes in the intensity of the porphyrins upon addition of MWCNT

Ground-state interactions between porphyrins and CBN can be influenced by the geometry of the latter. In this context, fGRAPH being partially planar should be more suitable for π-π interactions with the also planar porphyrins moiety, as compared to the tubular structures of the CNT. Moreover, the COOH groups present in the functionalized materials may sterically hinder π-π interactions. However, one must consider that for the aqueous systems, opposite charged porphyrins may also establish additional electrostatic interactions with the charged CBN (fCNT and fGRAPH). The fact that major spectral alteration occur in the case of fCNT and then fGRAPH confirms the importance of such interactions.

The excited-state interactions are primarily influenced by the reduction potential of CBN. According to previous reports in literature [18]–[20] the dynamic quenching involving these structures is due to a photoinduced electron transfer (PET) process between the electron donor, the porphyrin, and the electron acceptor, the CBN. The free energy change ΔG for PET depends on the oxidation potential of the donor, and the reduction potential of the acceptor. The lower the redox potential, the more PET process is favoured so that dynamic quenching is most efficient.

MWCNT contains mainly unsaturated sp^2 carbons and so the electron deficiency makes them better electron acceptors. In turn, fCNT, is heavily substituted by carboxyl groups, and so contains essentially sp^3 carbon atoms. Thus, making fCNT as the less efficient electron acceptor CBN used in this study. The case of fGRAPH is an intermediate one, since carboxyl functionalization occurs solely on the edges leaving the basal plane with its sp^2 carbon hybridization intact.

All together, data seems to indicate that the PET process is not the most efficient for either system studied and complexation is highly favourable for the functionalized CBN.

3.2 Porphyrin interaction with CNT decorated with gold

3.2.1 AuNP and AuNP/PEG with fCNT in water

TEM images of AuNP and AuNP/PEG with fCNT in water (not shown), prepared using the preformed method, showed contained both nanotubes as nanoparticles are present in the solution, but they did not interact with each other in both cases. A possible explanation for this is that these AuNP are too big to interact with these thin fCNT.

The alternative was to use (not functionalized) multiwall carbon nanotubes (MWCNT), which are wider and contain less strong π-π interactions, thus increasing the chance of interaction and making dispersion easier. Also, the system with PEG is preferred and solely used in the study involving MWCNT (see below).

3.2.2 AuNP/PEG with MWCNT in water/DMF mixtures

As said above, AuNP/PEG was introduced to MWCNT in two different ways: preformed and *in situ*, from which the TEM for the latter method is represented in figure 15 (the preformed method gave a similar image). Noticeable is that AuNP (2,B) and the MWCNT (3,B) did adsorb as expected because multiwall nanotubes are wider than single wall nanotubes, they have a width of approximately 8-21 nm [19]. The images show that the nanotubes have the tendency to aggregate together, whereas the particles are spread homogeneously. Both methods give a good interaction between nanotubes and nanoparticles, yet the preformed method gives a better dispersion, but both methods are used for further experiments.

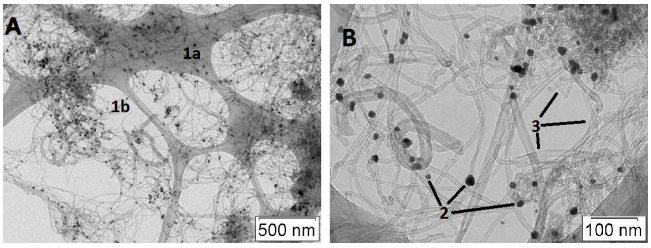

Fig. 15: TEM image of AuNP/PEG with MWCNT using the *in situ* method with A) a general image with a scale of 500 nm and B) a close up with a scale of 100 nm

A. *TMpyP*

UV/vis absorption of TMpyP using the 2 different methods, preformed and *in situ* (fig. 16(a)), showed no changes in the position (λ_{max} = 435 nm) or the shape of the bands, nor is there a formation of a new absorption band upon addition of AuNP/PEG/MWCNT. This result suggests no interaction occurred in the ground state between TMpyP and MWCNT decorated with gold, using either of the preparing methods.

Fluorescence intensity of TMpyP lowers significantly with increasing amount of AuNP/PEG/MWCNT, using the preformed and *in situ* method (fig. 16(b)). Besides this phenomenon, the spectra did not show a change in peaks (λ_{max} ~650 and ~712 nm for both A and B) and no new emission band was formed, suggesting no assembly occurred between porphyrin and MWCNT decorated with gold. The emission can be assigned to the free porphyrin monomers.

The quenching effect of both methods was taking into account using Eq.2.

Both methods give a lifetime on 11,2 ns for solely TMpyP. τ_{av} of TMpyP in the presence of AuNP is ~10,6 ns when using the *in situ* method of preparation, which is slightly shorter than using the preformed method (~11,1 ns), suggesting a better interaction of the two species adsorbed to MWCNT. Nonetheless, this difference is within the error of the experiment (10 %) and so a K_{SV} ~0 mL/mg was assumed for both cases of AuNP preparation. Regarding the static component, the association constants obtained are similar, K_a = 36.9 and 45.8 mL/mg, respectively, for preformed and *in situ* preparations. The latter is even identical to that obtained in the absence of AuNP.

Fluorescence decays of TMpyP with AuNP/PEG/MWCNT using either method were fitted using just one exponential. This result, together with the fluorescence spectra, indicates the same: TMpyP and MWCNT decorated with AuNP did not form an assembly in the excited state using either method.

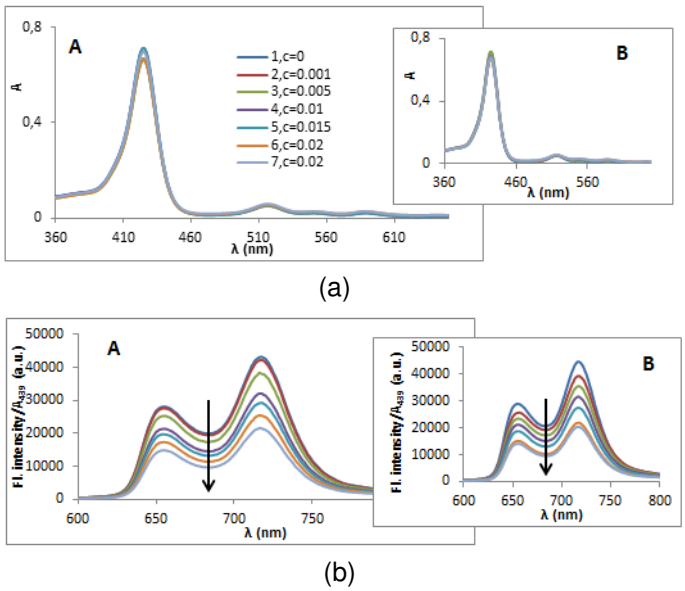

Fig. 16: (a) UV/vis absorption spectra and (b) fluorescence emission spectra (λ_{exc} = 439 nm) of TMpyP/water (2 μM) upon addition of AuNP/PEG/MWCNT in water-DMF (0-0,025 mg/ml) using the preformed method (A) and the *in situ* method (B)

B. *ZnTMpyP*

Upon addition of MWCNT decorated with AuNP no changes occurred in position (~439 nm) or shape of the bands in the UV/vis absorption spectra for neither of the two methods used, there are small insignificant changes in intensity (fig. 17(a)). For these reasons one can conclude neither the preformed nor the *in situ* method resulted in an assembly between ZnTMpyP and MWCNT decorated with AuNP.

Looking at the fluorescence emission spectra, there is a drop in in fluorescence intensity of ZnTMpyP/water upon addition of AuNP/PEG/MWCNT in water-DMF using the preformed and *in situ* method (fig. 17(b)). Whereas in the case of the preformed method there is a concomitant decrease of fluorescence intensity with increasing amounts of AuNP/PEG/MWCNT, for the *in situ* method a more heterogeneous dependence is detected. Neither A or B spectra changed regarding position or shape (λ_{max} ~632 and ~672 nm), nor did a new emission band form, suggesting the emission is only due to the free ZnTMpyP monomers, hence suggesting no assembly occurred between ZnTMpyP and MWCNT decorated with AuNP.

To obtain the rate constants for the quenching process, Eq. 2 was used once more. K_{SV} has a value of a 0 mL/mg for both the preformed as the *in situ* method. This is in agreement with the obtained lifetime data, where there is no dependence on [AuNP/PEG/MWCNT] for either method.

All the samples, both for the preformed method as for the *in situ* method, are fitted with one exponential and all have a constant lifetime value of ~1,52 ns, whether in the presence or in the absence of AuNP/PEG/MWCNT. This suggests that there is no dynamic quenching effect in either cases.

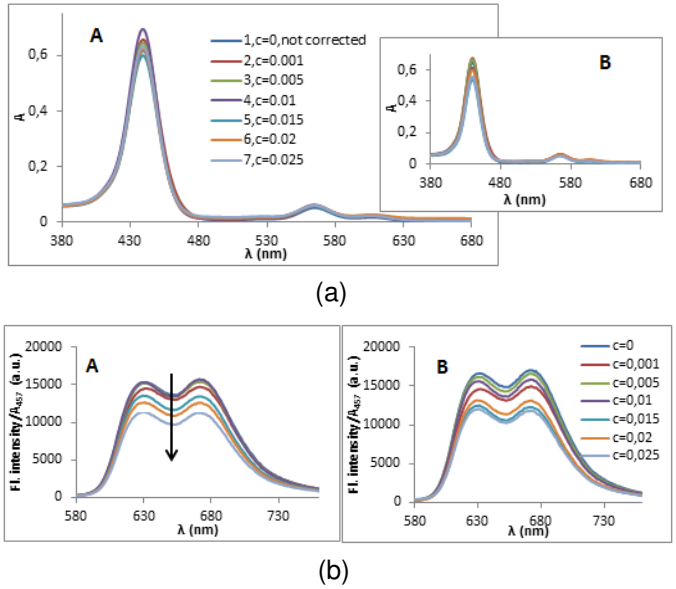

Fig. 17: (a) UV/vis absorption spectra and (b) fluorescence emission spectra (λ_{exc} = 457 nm) of ZnTMpyP/water (2 μM) upon addition of AuNP/PEG/MWCNT in water-DMF (0-0,025 mg/mL) using the preformed method (A) and the *in situ* method (B)

C. *Comparison*

Neither of the two porphyrins interacted with MWCNT decorated with AuNP the ground state, nor did they interact in the excited state. Based on K_{SV} values (table 4) and the plots of F_0/F to C (fig. 18), the sequence of the ability of the intensity quenching is TMpyP - *in situ* > TMpyP - preformed > ZnTMpyP - *in situ* > ZnTMpyP - preformed. This result indicates that the quenching effect of the AuNP/MWCNT system is more pronounced for TMpyP than ZnTMpyP and preparing AuNP *in situ* results in more quenching. TMpyP - *in situ*

is the only one with dynamic quenching effect, all others solely have a static quenching effect, i.e. in the ground state.

As for the static component, again the association constants obtained are within the same order of magnitude, 12.3 and 17.4 mL/mg, respectively for the preformed and the *in situ* methods. Noticeable, in this case they are both lower than those obtained for the system without AuNP.

TABLE 4: Stern-Volmer quenching constant K_{SV} and association constant K_a for different porphyrins and different preparing methods of AuNP/PEG/MWCNT

	TMpyP preformed	TMpyP *in situ*	ZnTMpyP preformed	ZnTMpyP *in situ*
K_{SV} (mL/mg)	0	0	0	0
K_a (mL/mg)	36,9	45,8	12,3	17,4

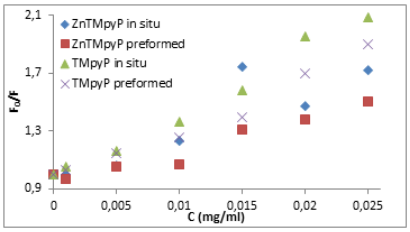

Fig. 18: The plot of intensity quenching upon the quencher concentration C for MWCNT decorated with AuNP

3.2.3 FLIM-images

A. *TMpyP*

In figure 19 it is depicted the data obtained with TMpyP. For the porphyrin alone (A) we see an almost homogeneous image with an τ_{av} of 3 ns which is shorter than that obtained for TMpyP free in aqueous solution probably due to some aggregation derived from solvent evaporation or even an interaction with the glass surface.

The interaction of TMpyP with MWCNT (B) causes fluorescence quenching with the τ_{av} of the porphyrin around 1.3 ns obtained by point measurement in the tubular region.

The effect of the addition of AuNP on TMpyP fluorescence depends on the method of preparation of NP (C): when preformed AuNP are added to the system there is a decrease of both fluorescence intensity and τ_{av}; whereas when AuNP are grown *in situ*, a huge increase of the fluorescence intensity is observed together with a shortening of τ_{av}. This last behaviour is indicative of a possible effect of metal enhanced fluorescence emission (MEF). This phenomenon can occur when the dye is located at suitable distances from the metal NP. It seems that in the case of the pre-formed NP the distance between dye and NP is not suitable for MEF. Probably, an electron transfer process may occur which leads to a quenching of both intensity and lifetime.

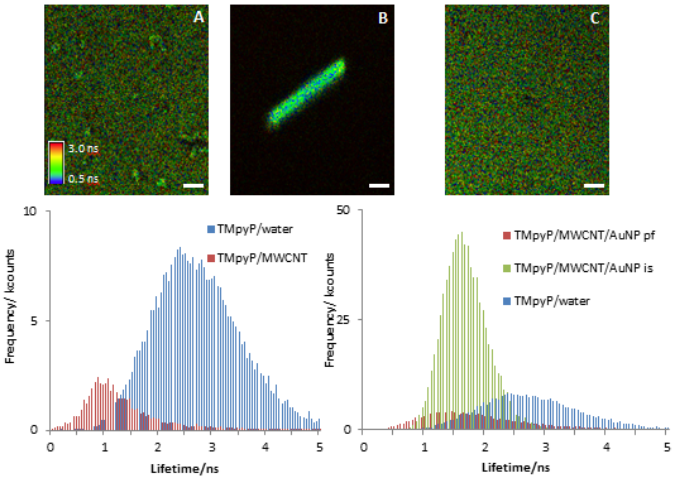

Fig. 19: FLIM images and respective lifetime histograms of TMpyP deposited from (A) an aqueous solution, (B) MWCNT (0.02 mg/mL), and (C) AuNP/PEG/MWCNT (0.025 mg/mL) prepared *in situ*. The lifetime scale is shown on the left. Image bar scale 10 μm.

B. *ZnTMpyP*

Data was also obtained using the metallated porphyrin, fig. 20. A homogeneous image was retrieved for the porphyrin deposited from an aqueous solution with an τ_{av} of 1.1 ns (A), which is only slightly shorter than that obtained for the porphyrin free in solution, thus ruling out aggregation during solvent evaporation.

The presence of fCNT (B) leads to a change in the histogram profile which shows a higher contribution from short lifetimes as compared to water.

Upon addition of AuNP/MWCNT/PEG, we see a more heterogeneous image (but similar for the two different method of NP preparation) but with quite a distinct histogram: in both cases there is a shortening of the fluorescence lifetimes and an increase in fluorescence intensity as compared to the dye alone. However, the enhancement is far more intense when the *in situ* method is used to obtain AuNP. The fact that NP spreading seems to be better reached for the latter method, may contribute to ensure dye-AuNP interaction and thus leading to a statistically measurable effect of MEF.

4 Conclusion

It was possible to design porphyrin/fCNT nanohybrids, from which the properties were studied using UV/vis absorption, steady state and time-resolved spectroscopy, as well as by FLIM. The CBN fGRAPH and MWCNT did not result in the same. Differences between CBN can be assigned to their differences in geometry, which influences ground-state interaction, and in reduction potential, which influences interactions in the excited state.

Also, no hybrid systems could be made using MWCNT decorated with gold, using either the preformed preparing method or the *in situ* method in solution.

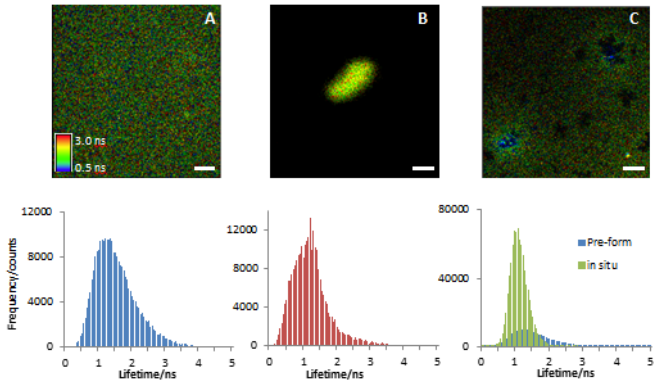

Fig. 20: FLIM images and respective lifetime histograms of ZnTMpyP deposited from (A) an aqueous solution, (B) fCNT (0.025 mg/mL), and (C) AuNP/PEG/MWCNT (0.025 mg/mL) prepared *in situ*. The lifetime scale is shown on the left. Image bar scale 10 μm.

Although no differences could be distinguished between the two methods based on the spectroscopic results, FLIM images did show a distinction: with the addition of preformed AuNP fluorescence quenching of the porphyrin is obtained, whereas for the *in situ* prepared AuNP an increase of the porphyrin fluorescence intensity together with a decrease of its lifetime was observed, which is characteristic for the MEF effect.

REFERENCES

[1] S. Andrade, "Metal nanoparticles growth on carbon nanostructures with photoactive molecules towards optoelectronic applications," 2013-2014.

[2] X.-F. Zhang and X. Shao, "π–π binding ability of different carbon nano-materials with aromatic phthalocyanine molecules: Comparison between graphene, graphene oxide and carbon nanotubes," *Journal of Photochemistry and Photobiology A: Chemistry*, vol. 278, pp. 69–74, 2014.

[3] J. Sessler, E. Karnas, E. Sedenberg, P. Gale, and J. Steed, "Supramolecular chemistry: From molecules to nanomaterials," 2012.

[4] R. Boscencu and others., "Biomedical Engineering - From Theory to Applications," 2011.

[5] G. M. J. and others., "Chemical Communications," pp. 4145–4162, 2012.

[6] C. Alejo, private communication, 2014.

[7] D. M. Togashi and S. M. Costa, "Absorption, fluorescence and transient triplet–triplet absorption spectra of zinc tetramethylpyridylporphyrin in reverse micelles and microemulsions of aerosol ot–(aot)," *Physical Chemistry Chemical Physics*, vol. 2, no. 23, pp. 5437–5444, 2000.

[8] S. M. Andrade and S. Costa, "Spectroscopic studies of water-soluble porphyrins with protein encapsulated in bis (2-ethylhexyl) sulfosuccinate (aot) reverse micelles: Aggregation versus complexation," *Chemistry-A European Journal*, vol. 12, no. 4, pp. 1046–1057, 2006.

[9] TCI, "Products, TCI America," "www.tcichemicals.com/eshop/pt/br/commodity/A5012/".

[10] R. Correia, "Cell membrane models made up from amphiphiles and proteins," Ph.D. dissertation, IST, Lisbon, Portugal, 2012.

[11] M. A. Castanho, N. C. Santos, and L. M. Loura, "Separating the turbidity spectra of vesicles from the absorption spectra of membrane probes and other chromophores," *European biophysics journal*, vol. 26, no. 3, pp. 253–259, 1997.

[12] H. J. Y. Inc., *Fluorolog® Tau-3 lifetime system - Operation manual*, Germany, 2001.

[13] M. R. Eftink and C. A. Ghiron, "Fluorescence quenching studies with proteins," *Analytical biochemistry*, vol. 114, no. 2, pp. 199–227, 1981.

[14] G. Behera, B. Mishra, P. Behera, and M. Panda, "Fluorescent probes for structural and distance effect studies in micelles, reversed micelles and microemulsions," *Advances in colloid and interface science*, vol. 82, no. 1, pp. 1–42, 1999.

[15] P. Kubát, K. Lang, P. Janda, O. Frank, I. Matulková, J. Sỳkora, S. Civiš, M. Hof, and L. Kavan, "Self-assemblies of cationic porphyrins with functionalized water-soluble single-walled carbon nanotubes," *Journal of nanoscience and nanotechnology*, vol. 9, no. 10, pp. 5795–5802, 2009.

[16] F. J. Vergeldt, R. B. Koehorst, A. van Hoek, and T. J. Schaafsma, "Intramolecular interactions in the ground and excited states of tetrakis (n-methylpyridyl) porphyrins," *The Journal of Physical Chemistry*, vol. 99, no. 13, pp. 4397–4405, 1995.

[17] S. M. Andrade and S. Costa, "Spectroscopic studies on the interaction of a water soluble porphyrin and two drug carrier proteins," *Biophysical journal*, vol. 82, no. 3, pp. 1607–1619, 2002.

[18] S. M. Andrade, P. Raja, V. K. Saini, A. S. Viana, P. Serp, and S. Costa, "Polyelectrolyte-assisted noncovalent functionalization of carbon nanotubes with ordered self-assemblies of a water-soluble porphyrin," *ChemPhysChem*, vol. 13, no. 16, pp. 3622–3631, 2012.

[19] S. P., Toulouse, France, responsible for the synthesis.

[20] J. Malig, N. Jux, and D. M. Guldi, "Toward multifunctional wet chemically functionalized graphene integration of oligomeric, molecular, and particulate building blocks that reveal photoactivity and redox activity," *Accounts of chemical research*, vol. 46, no. 1, pp. 53–64, 2012.